THE JOURNAL OF PHYSICAL CHEMISTRY A
A JOURNAL OF THE AMERICAN CHEMICAL SOCIETY

pubs.acs.org/JPCA

Article

Sensitization of Nd^{3+} Luminescence by Simultaneous Two-Photon Excitation through a Coordinating Polymethinic Antenna

Jesús Durán-Hernández, Leonardo Muñoz-Rugeles, Óscar Guzmán-Méndez, Mariana M Reza, Andrea Cadena-Caicedo, Verónica García-Montalvo, and Jorge Peón*

Cite This: J. Phys. Chem. A 2022, 126, 2498−2510

Read Online

ACCESS | Metrics & More | Article Recommendations | Supporting Information

ABSTRACT: We have designed and synthesized two new cyaninic Nd^{3+} complexes where the lanthanide emission can be induced from simultaneous two-photon absorption followed by energy migration. These complexes correspond to a molecular design that uses an antenna ligand formed by the functionalization of a heptamethine dye with 5-ol-phenanthroline or 4-phenyl-terpyridine derivatives. These complexes employ the important nonlinear optical properties of symmetric polymethines to sensitize the lanthanide ion. We verified that simultaneous biphotonic excitation indirectly induces the $^4F_{3/2} \rightarrow {}^4I_{11/2}$ Nd^{3+} emission using femtosecond laser pulses tuned below the first electronic transition of the antenna. The simultaneous two-photon excitation events initially form the nonlinear-active second excited singlet of the polymethine antenna, which rapidly evolves into its first excited singlet. This state in turn induces the formation of the emissive Nd^{3+} states through energy transfer. The role of the first excited singlet of the antenna as the donor state in this process was verified through time resolution of the antenna's fluorescence. These measurements also provided the rates for antenna-lanthanide energy transfer, which indicate that the phenanthroline-type ligand is approximately five times more efficient for energy transfer than the phenyl-terpyridine derivative due to their relative donor−acceptor distances. The simultaneous two-photon excitation of this polymethine antenna allows for high spatial localization of the Nd^{3+}excitation events.

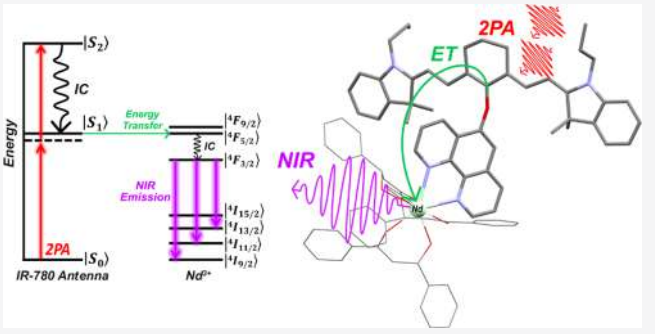

INTRODUCTION

Lanthanide ions produce long-lived luminescence that makes them useful in applications ranging from optoelectronic devices to biological fluorescent probing.[1−8] Lanthanide ions, however, have extremely small molar absorptivities of the order of 10 M^{-1} cm^{-1}. A method to overcome such a low photon capture efficiency is by coordinating these ions with organic chromophores with much larger absorption coefficients.[9−11] The use of organic chromophores is based on sensitization schemes that indirectly populate the excited states of lanthanide ions.[1,2,9,10] Energy transfer in these systems can occur in two ways: through the electronic exchange mechanism and/or the Coulombic-multipolar mechanism.[12−17] From the distance dependence of these processes, greater efficiency for the energy migration is achieved if the organic chromophore is coordinated directly to the lanthanide ion.[18−22]

Among the chromophores that have been used as molecular antennas in these applications are cyanine dyes due to their high molar absorptivities and excellent photochemical properties.[23−26] Cyanines have also been of great interest due to their nonlinear optical properties, which in turn arise from their symmetry and extended conjugation.[27−32] These dyes are also frequently used in biological applications, including cell imaging,[33−38] and as antenna groups for light up-conversion in nanoparticles.[39−44] The chemical versatility of cyanines and other polymethinic systems comes from the fact that they can be easily functionalized in ways that conserve their electronic and optical properties.[45−49]

In this contribution, we present the synthesis and characterization of two Nd^{3+} complexes where the ion can be sensitized through simultaneous two-photon absorption by a polymethine antenna. Nonlinear activation of emissive or photochemically active systems allows for optical control of molecules at a variable depth in a sample or tissue through the use of appropriate focusing optics.[50−55] From the intensity dependence of two-photon absorption, in these systems, the volume where the excited states are formed can be defined with a precision of the order of a femtoliter.[56−59] Such spatial control is relevant in cases where the excitation needs to take

Received: February 12, 2022
Revised: March 31, 2022
Published: April 18, 2022

Downloaded via UNIV NACIONAL AUTONOMA MEXICO on February 5, 2025 at 22:13:35 (UTC).
See https://pubs.acs.org/sharingguidelines for options on how to legitimately share published articles.

ACS Publications
© 2022 American Chemical Society

https://doi.org/10.1021/acs.jpca.2c01052
J. Phys. Chem. A 2022, 126, 2498−2510

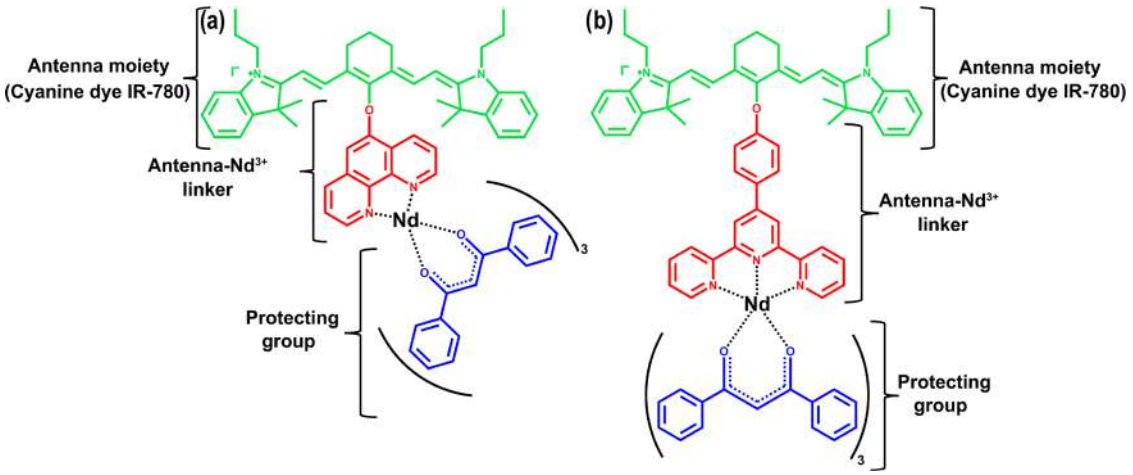

Figure 1. Chemical structures of (a) IR-phenNd(DBM)$_3$ and (b) IR-tpyNd(DBM)$_3$.

place in a small volume inside a biological sample or when a photochemical process needs to be initiated below the surface of a material.[60−62]

As shown in Figure 1, in this contribution, we studied antenna-lanthanide complexes, which result from the functionalization of the IR-780 cyanine with phenanthroline or phenyl-terpyridine derivatives, which in turn can coordinate with metallic ions.[63−66] This allows for a close interaction between the ion and the organic antenna. A key aspect of the complexes in Figure 1 is the fact that the IR-780 antenna has a higher singlet excited state (S_2), which can be populated nonlinearly, thanks to its large two-photon absorption coefficient of up to 2800 GM at 875 nm.[67,68] Such large cross section results from the symmetry properties of this state and a near coincidence of: (1) The first cyaninic transition of 1.5 eV and (2) an S_1-S_2 energy gap of 1.3 eV. With these energy differences, the polymethine chain can be efficiently excited through simultaneous two-photon excitation in the 800−900 nm region. This scheme has been described in previous publications by our group and used in two-photon antenna schemes to induce indirect photoisomerization or photodissociation of organic effectors through a nonlinear optical process.[47,48]

As shown below, we first demonstrate that the polymethinic ligands are capable of transferring energy to the Nd^{3+} ion from their first excited singlet localized in the cyanic antenna after regular linear excitation into the intense 780 nm band of the polymethinic chain.[69] This by itself is relevant since it corresponds to an efficient linear sensitization scheme, which uses one of the largest absorption coefficients among organic chromophores (274,000 M^{-1} cm^{-1} at 780 nm). The sensitization of lanthanide emission after excitation into this band, with energy transfer occurring from the fluorescent singlet, is in itself noteworthy since in most lanthanide complexes, the energy transfer takes place from a triplet state. This kind of sensitization is also frequently set up to occur through intraligand charge transfer states (^{1}ILCT).[70−75] The present scheme differs from the abovementioned ones as it involves directly the first singlet excited state of cyanine, which has an excellent overlap integral for energy transfer with the $^4F_{5/2} \leftarrow {}^4I_{9/2}$ transition of the Nd^{3+} ion (see below).

Cyanine-sensitized lanthanide complexes have been studied previously. A related system corresponds to the recent contribution by Golesorkhi et al., who synthesized an Er^{3+} complex based on a cyanine dye antenna functionalized with a bis(benzimidazole)pyridine unit with a sulfur bridge. The authors demonstrated energy up-conversion associated with the induction of Er^{3+} emissions at 522 and 542 nm.[76] Such scheme, however, differs from the one in the present contribution in that, for our scheme, the sensitization is done through simultaneous two-photon excitation with light pulses tuning below the first antenna transition rather than the 1 + 1 excitation scheme of Golesorkhi et al., which does not have the spatial or intensity dependence of simultaneous two-photon absorption. Other cases that involve the sensitization of the Er^{3+} ion with cyanines are the systems formed by ionic pairs with these dyes. The first of them was reported by Hyppänen, where the authors used the IR-806 cyanine as an antenna, showing that the Er^{3+} emission at 510−565 nm was produced by a similar 1 + 1 up-conversion process.[77] Finally, Yang and Qian demonstrated the NIR luminescence at 1500 nm of the Er^{3+} ion by energy transfer from the IR-140 cyanine dye, again, after regular linear excitation.[78]

For the present contribution, we connected the Nd^{3+} ion to the cyanine antenna using phenanthroline (OH-phen) or phenyl-terpyridine (OH-tpy) fragments as shown in Figure 1. The phenyl-terpyridine system is similar to the Er^{3+} complex by Golesorkhi et al. since it uses a phenyl-terpyridine-type ligand, but with an oxygen bridge instead of a bis(benzimidazole)pyridine ligand with a sulfur bridge. As shown below, the phenanthroline-type ligand of this contribution was considered since it can significantly increase the yield of energy transfer thanks to a smaller donor−acceptor distance. In addition, the current complexes take into account the protection of the lanthanide ion through the additional coordination of 1,3-diphenyl-1,3-propanedione (HDBM) units. Since lanthanide ions are highly oxyphilic,[10] these ligands contribute to the protection of the Nd^{3+} ion from the solvent environment, hence reducing the quenching of the excited states so that the lanthanide emission can be detected.

SYNTHESIS, MATERIALS, AND METHODS

Steady-State, Biphotonic, and Time-Resolved Spectroscopies. UV−vis absorption spectra were recorded on a Cary-50 spectrophotometer (Varian) and the emission and excitation spectra on a Cary Eclipse fluorometer (Varian). All spectra were recorded at room temperature (21 °C). The NIR Nd^{3+} emission spectra resulting from simultaneous two-photon

https://doi.org/10.1021/acs.jpca.2c01052
J. Phys. Chem. A 2022, 126, 2498−2510

Scheme 1. General Synthesis for Nd^{3+} Complexes: (A) H_2SO_4 (90−97%)/H_2O, t = 2 h, Reflux, NaOH, pH = 7;[80,81] (B) EtOH/H_2O/NH_3, t = 24 h at T = 0 °C;[82,83] (C) Acetonitrile/Et_3N, t = 48 h, Room Temperature;[47−49] (D) $Nd(NO_3)\cdot 6H_2O$, Acetone/H_2O/NH_3, t = 15 min, Room Temperature;[84,85] and (E) Acetone, t = 36 h, Room Temperature[84,85]

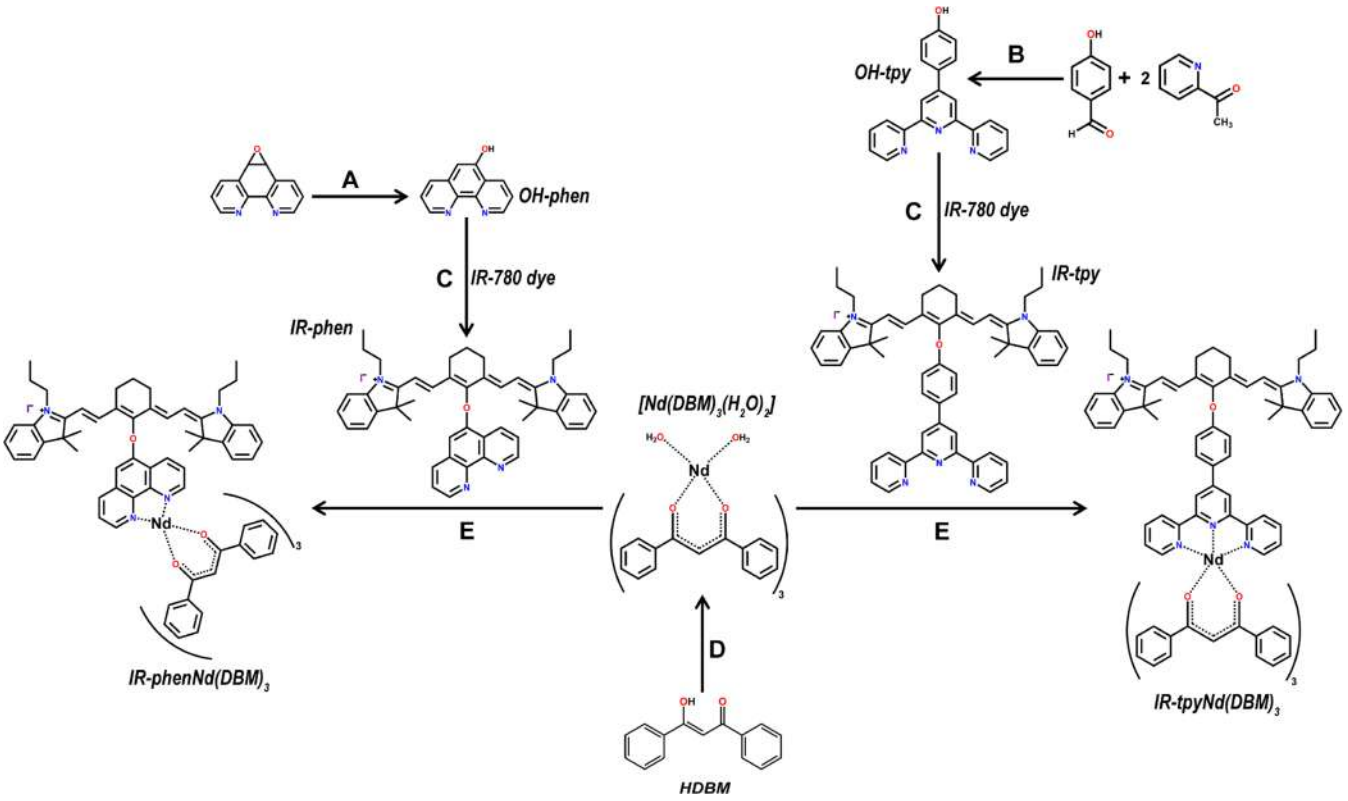

absorption were obtained by excitation with a femtosecond laser centered at 865 nm (energetically below the first cyaninic transition) for nonlinear optical excitation. The pulse duration in the beam was of 110 fs. The average power was attenuated to the order of 1 mW or less with a 1 kHz repetition rate. The two-photon excitation beam was focused to a 0.5 mm waist spot at the sample with a microscope objective of 1 cm focal length (Melles Griot). The complexes were studied in a 1 cm cell under constant stirring. The emission was collected and collimated by a 1 cm focal length parabolic mirror and then refocused into the detection system with a 15 cm focal length lens. The emission spectra in the 1000−1100 nm region were acquired using a scanning monochromator (SCIENCETECH MODEL 9050) and a Si photodiode from THORLABS, model DET10A (200−1100 nm). A detailed diagram is included in the Supporting Information, also describing the detection method.

The excited-state lifetimes of the ligands and the respective fluorescence anisotropy decays were obtained by the time-correlated single-photon counting (TCSPC) technique using a picosecond pulsed laser (LDH-D-C-405, 405 nm) for excitation.[48] The fluorescence was collected through the same reflective objective of 7.8 mm working distance, filtered with a dichroic mirror, and focused into an avalanche photodiode (PD-050-CTE, Micro PhotonDevices) connected to a TCSPC system (PicoHarp 300, PicoQuant). The Instrument Response Function (IRF) was obtained by the method described by Liu *et al.*[79] Briefly, a 100 mM phosphate buffer (pH = 10) was used to prepare a saturated 12 M NaI solution. A saturated sodium fluorescein solution was then prepared by progressively adding the saturated NaI solution until the fluorescein was completely dissolved. The rapid decaying emission from this solution was taken as the IRF of our setup. The TCSPC traces were fitted to exponential decays convoluted with the IRF using the SymPhoTime software from PicoQuant.

Synthesis of Nd^{3+} Complexes. Scheme 1 shows the general synthetic path to obtain the cyaninic Nd^{3+} complexes. Details of the synthesis and characterization are included in the Supporting Information.

Computational Methods. The ground-state equilibrium geometries of the polymethinic ligands were obtained through the DFT method to estimate center-to-center distances between the antenna section and the Nd^{3+} ion. For the calculations, the Gaussian16[86] set of programs were used, considering the PBE0/6-311++G(d,p) level theory using the polarizable continuum model (PCM) solvation model for ethanol and acetone.

RESULTS AND DISCUSSION

Spectroscopies of the IR-780 Dye and the Nd^{3+} Ion. The absorption spectrum of the IR-780 dye extends across the UV−vis−NIR region as shown in Figure 2. It exhibits a series of small bands in the 250−500 nm region, which are associated with higher excited states of polymethine chains.[47−49,67,68,87] The most prominent signal is in the 600−850 nm region and corresponds to the first singlet excited state. This band has a high molar absorptivity coefficient of 274,000 M^{-1} cm^{-1}.[47−49,67,68] On the other hand, several of the higher excited states (S_n (n > 1)) are partially prohibited by one-photon absorption,[29,47−49,67,68,87] which results in low absorption peaks in the region below the first transition

https://doi.org/10.1021/acs.jpca.2c01052
J. Phys. Chem. A 2022, 126, 2498−2510

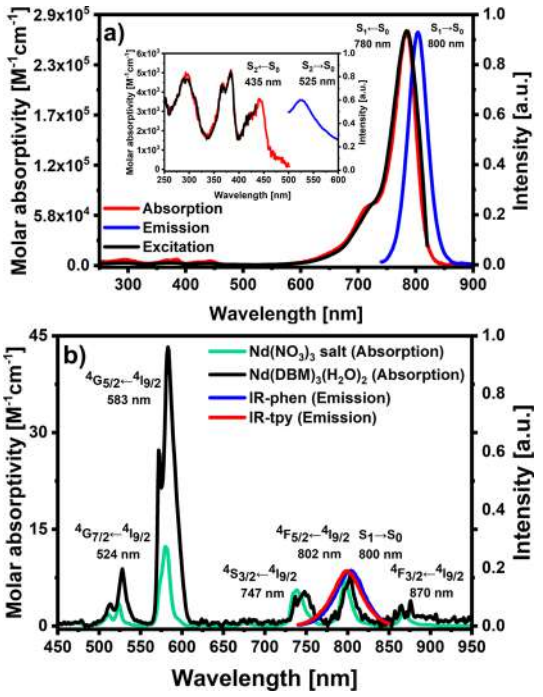

Figure 2. (a) Absorption (red line), emission (blue line, λ_{exc} = 730 nm), and excitation (black line) (λ_{em} = 800 nm) spectra of the IR-780 dye. Inset: absorption (red line), emission (blue line, λ_{exc} = 435 nm), and excitation (black line, λ_{em} = 525 nm) spectra of the higher excited states. The emission spectrum of the S_2 state is centered at 525 nm. (b) Absorption spectra of Nd^{3+} nitrate (green line) and $Nd(DBM)_3(H_2O)_2$ (black line) solutions and emission (λ_{exc} = 730 nm) from the S_1 state of the IR-phen (blue line) and IR-tpy (red line) ligands. All spectra were obtained at room temperature in high-performance liquid chromatography (HPLC) ethanol.

wavelength. As mentioned in the introduction, the S_2-S_1 gap is 1.3 eV in this cyanine. As a result of this large gap, the excited state S_2 is slightly fluorescent and its emission is centered at 525 nm.[29,47−49,67,68,87] As a key element of the present design, several of the S_n, $n > 1$ states, have important two-photon absorption cross sections, with a peak of 2800 GM units at 875 nm.[67,68] This feature implies that the cyaninic S_2 singlet can be efficiently populated with NIR pulses from an appropriately tuned Ti:Sapphire laser. This is the basis of the present Nd^{3+} biphotonic sensitization scheme.[29,47,48,67,68,87]

To formulate a suitable exciton migration mechanism, certain conditions must be met for the coupling between the antenna and the Nd^{3+} states. As can be seen in Figure 2b, there is an excellent match between the $^4F_{5/2} \leftarrow {}^4I_{9/2}$ band of the ion and the emission band of the first excited singlet of the cyanine ligands. Hence, it can be suggested that energy transfer can occur from the first excited singlet state of the IR-780-type antenna to the $^4F_{5/2}$ state of the ion (this was verified by time-resolving the emission from the antenna section, see below).

Steady-State Spectroscopy of IR-phen and IR-tpy Ligands. The absorption spectra of IR-phen and IR-tpy ligands show the characteristic bands of each segment that form the ligands. The region below 350 nm shows the features of the phenanthroline and phenyl-terpyridine fragments within the ligands. The respective absorption, emission, and excitation spectra of these molecules are shown in the Supporting Information. The 350−500 nm region shows several of the smaller bands associated with the higher excited states of the cyaninic section. Again, the strongest absorption band corresponds to the S_1 excited state of the IR-780 chromophore. As can be seen, the way the ligands bind to the antenna allow for each section to retain their locally defined nature and ordering in the spectrum. This is demonstrated in Figure 3

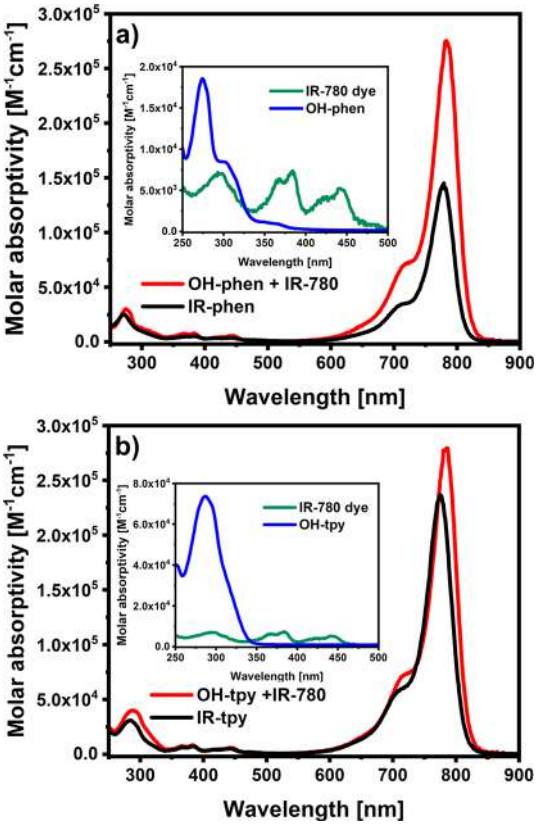

Figure 3. (a) UV−vis−NIR absorption spectra of IR-phen (black line) and sum of the absorption coefficients of OH-phen and the IR-780 dye (red line). Inset: absorption spectra of OH-phen (blue line) and the IR-780 dye (green line) in the region below 500 nm. (b) UV−vis−NIR absorption spectra of IR-tpy (black line) and sum of the OH-tpy and IR-780 dye spectra (red line) based on their absorption coefficients. Inset: absorption spectra of OH-tpy (blue line) and IR-780 dye (green line) in the region below 500 nm. The spectra were obtained at room temperature in HPLC ethanol.

where we compare the spectra of the ligands with the sum of the spectra of the individual sections. Here, it is important to emphasize that the polymethinic sections in the ligands retain the character and symmetry properties for each state, which is essential to ensure that the IR-780 fragment maintains its high two-photon absorption cross section. As we have shown in previous contributions, this is a central element in these designs, which is achieved through the ether-type connectivity between the polymethinic chains and the phenyl-terpyridine or phenanthroline sections.[47−49] Also, the excitation spectra reproduce the profiles of the absorption spectra of both sections upon detection of the ligand's emission, as can be seen in Figure 4.

Spectroscopy of $Nd(DBM)_3(H_2O)_2$. Next, we describe the Nd^{3+} complex formed only with the HDBM ligands to differentiate its features from those of the final complexes. DBM is an auxiliary ligand that can keep the Nd^{3+} ion reasonably protected from the O−H solvent oscillators, allowing for a sufficient excited-state lifetime to detect the

https://doi.org/10.1021/acs.jpca.2c01052
J. Phys. Chem. A 2022, 126, 2498−2510

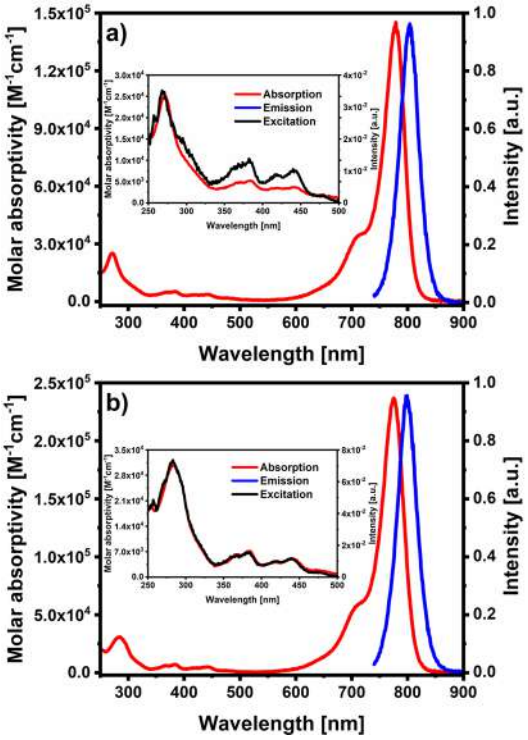

Figure 4. Absorption (red line), emission (blue line, λ_{exc} = 730 nm), and excitation (black line, λ_{em} = 800 nm) spectra of (a) IR-phen and (b) IR-tpy. Insets: Absorption (red line) and excitation (black line) spectra in the 250−550 nm region showing the features of the higher excited states of the polymethinic chain. The spectra were obtained at room temperature in HPLC ethanol.

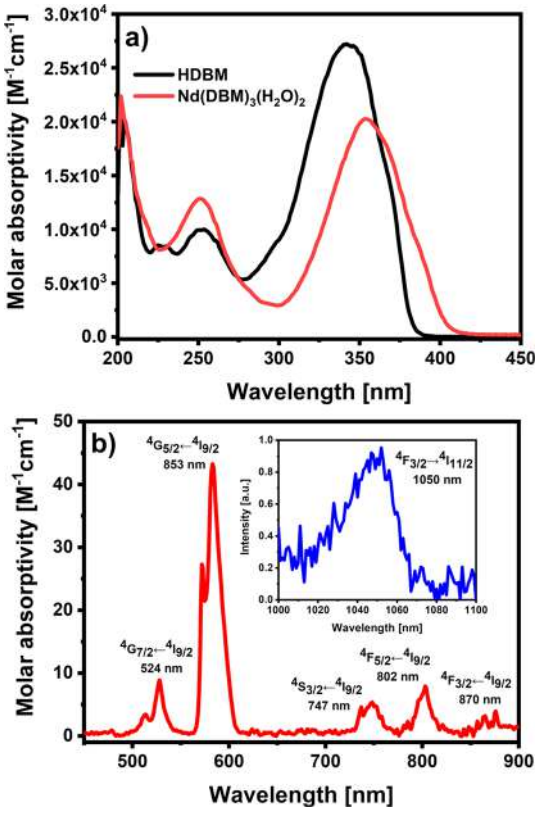

Figure 5. (a) Absorption spectra of HDBM (black line) and $Nd(DBM)_3(H_2O)_2$ (red line). (b) UV−vis−NIR absorption spectrum of a $Nd(DBM)_3(H_2O)_2$ solution (red line) in the visible and NIR region. Inset: emission of $Nd(DBM)_3(H_2O)_2$ (blue line) upon excitation at 800 nm. The spectra were obtained in HPLC ethanol.

Nd^{3+} luminescence.[9,10] The UV−vis spectrum of a HDBM solution shows a maximum centered at 342 nm, which is attributed to a $\pi^* \leftarrow \pi$ transition.[88] The $Nd(DBM)_3(H_2O)_2$ sample shows a reduction in the absorption coefficient and a red shift of this band that is now centered at 354 nm, as shown in Figure 5. Also, as expected, the $Nd(DBM)_3(H_2O)_2$ solutions exhibit the respective intraconfigurational transitions of the Nd^{3+} ion. Upon direct excitation at 800 nm ($^4F_{5/2} \leftarrow {}^4I_{9/2}$ transition), the characteristic emission of the Nd^{3+} ion was detected at 1050 nm, indicating the effectiveness of the ligands to partially protect the emissive $^4F_{3/2}$ state from quenching by the solvent. The $Nd(DBM)_3(H_2O)_2$ sample was excited at 354 nm and it was verified that no antenna effect is induced by the DBM ligands.

Photophysics of Cyanine−Nd^{3+} Complexes with Linear Excitation at 780 nm. The absorption spectra of the full complexes: IR-phen$Nd(DBM)_3$ and IR-tpy$Nd(DBM)_3$ are shown in Figure 6 and exhibit the characteristic bands of each of the molecular units. The regions below 350 nm show the signals from the phenanthroline and terpyridine sections. In the 300−400 nm range, the absorption features correspond to the DBM protecting ligands. The features in the 400−500 nm range correspond to the higher excited states of the IR-780 dye. As projected, the prominent band around 780 nm is preserved for the first excited state of the polymethine antenna. We notice that this antenna band decreases its absorptivity (as in the case of free ligands), most likely due to small changes in the planarity of the polymethinic chain.[87,102] As mentioned previously, it is important that the symmetry of the excited states is preserved since this is directly related to their nonlinear absorption properties.[47,48,67,68] These bands remain present in both IR-phen$Nd(DBM)_3$ and IR-tpy$Nd(DBM)_3$ in the region around 440 nm. In Figure 6, we include vertical arrows to indicate the wavelength of the femtosecond two-photon excitation pulses for the main experiments (865 nm, see below). It should be noted that the maximum two-photon absorbance of the IR-780 chromophore lies at 875 nm;[67] however, this wavelength is not within the reach of our Ti:Sapphire laser system. The two-photon absorption coefficient at 865 nm can be interpolated from the data in ref 67 to be ∼965 GM.

The emission spectra of the IR-phen$Nd(DBM)_3$ and IR-tpy$Nd(DBM)_3$ complexes were recorded by exciting the systems in the prominent 780 nm cyanine absorption (regular linear optical excitation). These Nd^{3+} complexes exhibit a clear emission band at 1050 nm. This band is typical of the emission of this lanthanide ion and is shown in the insets of Figure 7. For this ion, frequently, three emission bands are observed: $^4F_{3/2} \rightarrow {}^4I_{9/2}$ at 890 nm, $^4F_{3/2} \rightarrow {}^4I_{11/2}$ at 1050 nm, and $^4F_{3/2} \rightarrow {}^4I_{13/2}$ at 1350 nm.[9,10,89−91] We only observe the band centered at 1050 nm since the first band is masked by the emission of the antenna, and the third one is not within our instrumental detection reach.

The excitation spectra for both complexes are shown in Figure 7 and are obtained by detecting the sensitized lanthanide emission at 1050 nm. The scaled excitation spectra have a good match with the absorption profiles of the IR-phen and IR-tpy ligands. As expected, the band associated with the DBM ligand is absent. This shows that Nd^{3+} sensitization is

https://doi.org/10.1021/acs.jpca.2c01052
J. Phys. Chem. A 2022, 126, 2498−2510

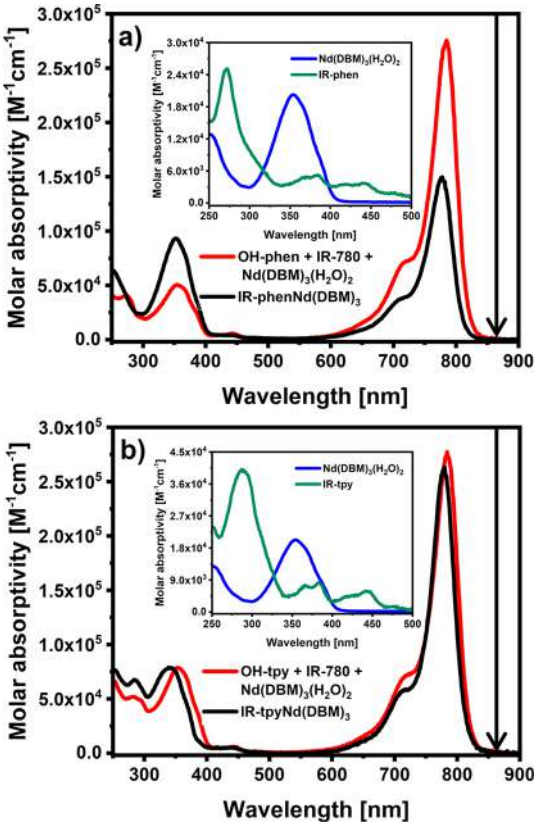

Figure 6. (a) Absorption spectra of IR-phenNd$(DBM)_3$ (black line) and sum of the spectra from OH-phen, IR-780, and Nd$(DBM)_3(H_2O)_2$ (red line). Inset: absorption spectra of Nd$(DBM)_3(H_2O)_2$ (blue line) and the IR-phen ligand (green line). (b) Absorption spectra of IR-tpyNd$(DBM)_3$ (black line) and the sum of OH-tpy, IR-780, and Nd$(DBM)_3(H_2O)_2$ (red line). Inset: absorption spectra of Nd$(DBM)_3(H_2O)_2$ (blue line) and the IR-tpy ligand (green line). The spectra were obtained in HPLC ethanol. The arrows indicate the wavelength for two-photon excitation used in our experiments (see below).

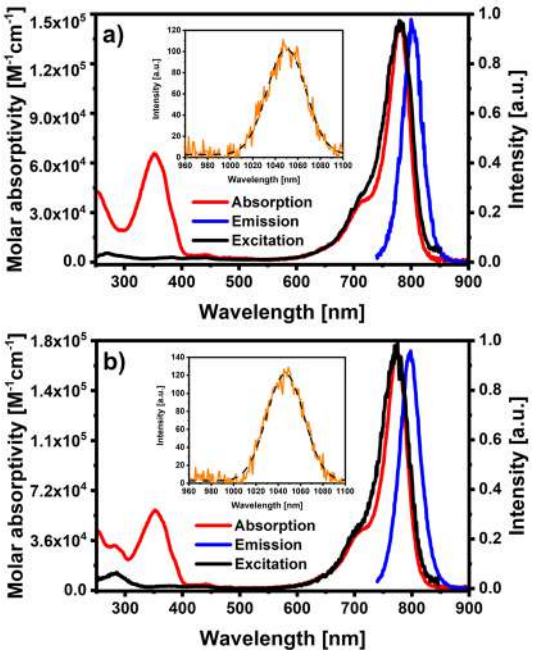

Figure 7. (a, b) Absorption (red line), emission (blue line, λ_{exc} = 730 nm), and excitation (black line, λ_{em} = 1050 nm) spectra of IR-phenNd$(DBM)_3$ and IR-tpyNd$(DBM)_3$. Insets: emission spectra (orange line, λ_{exc} = 780 nm) from the Nd^{3+} ion in the complex after baseline correction. The dashed black lines correspond to fits of the bands to Gaussian functions. The spectra were obtained from HPLC ethanol solutions.

being carried out from the IR-780 fragment without any participation of the DBM ligands. As can be seen, the excitation in the region of the first cyaninic transition allows for efficient linear sensitization of the lanthanide emission with the advantage of the 274,000 M^{-1} cm^{-1} polymethinic absorption coefficient at 780 nm. Different applications can be envisioned from regular linear absorption with such significant absorptivity in the NIR region.[5,6,10]

The sensitization of the Nd^{3+} emission across the polymethine antenna spectrum is a crucial verification of the potential of our biphotonic excitation scheme. Specifically, the experiments in Figure 7 demonstrate that once the organic antenna is excited to the higher states (S_n, $n > 1$), energy migration events result in the formation of Nd^{3+}-localized excited states. Here, the photophysical first step would correspond to internal conversion to form the antenna-localized S_1 state, and the second step, to energy transfer to the Nd^{3+} center.

Photophysics of Nd^{3+}–Polymethine Complexes upon Biphotonic Excitation with 865 nm Femtosecond Pulses. We detected the lanthanide ion emission after two-photon excitation using 110 fs, 865 nm laser pulses. The respective spectra are shown in Figure 8 for both complexes. The emission spectra were obtained with photon energies tuned below the first cyaninic transition as indicated with arrows in Figure 6. These emissions exhibit the characteristic band from the Nd^{3+} ion corresponding to the $^4F_{3/2} \rightarrow {}^4I_{11/2}$ transition at 1050 nm, which is also observed using linear excitation as in Figure 7. To verify the biphotonic nature of the 865 nm excitation of both Nd^{3+} complexes, we studied the dependence of the 1050 nm emitted intensity as a function of the power of the femtosecond pulse train. The log–log plot of the signal intensity as a function of the excitation average power shows slopes of ~2.3, which confirms that the lanthanide emissions are produced by nonlinear absorption by the cyanine antenna. The laser power interval we explored is limited on the lower end by the detection of the Nd^{3+} emission with our setup, and on the higher end, to the possibility of inducing other nonlinear optical effects, including self-phase modulation. Importantly, the control experiments of the Nd$(DBM)_3$ solutions without the antenna ligand did not show the 1050 nm band.

Time-Resolved Spectroscopy and Fluorescence Anisotropy Decays. The emission decays from the cyanine S_1 states of the complexes were followed using the TCSPC technique. Changes in the decays of these signals, comparing the free ligands with the Nd^{3+} complexes, give a direct measure of the energy transfer rates. The experiments were conducted by irradiating the solutions with 405 nm, 200 ps pulses and time-resolving the 800 nm antenna emissions in acetone solutions at room temperature. These experiments were carried out in acetone, while the previous Nd^{3+} emission experiments were performed in ethanol due to the fact that in acetone there is a more rapid formation of the complexes upon addition of Nd^{3+} aliquots. The static spectra in acetone are included in the Supporting Information. We carried out time-resolved

https://doi.org/10.1021/acs.jpca.2c01052
J. Phys. Chem. A 2022, 126, 2498–2510

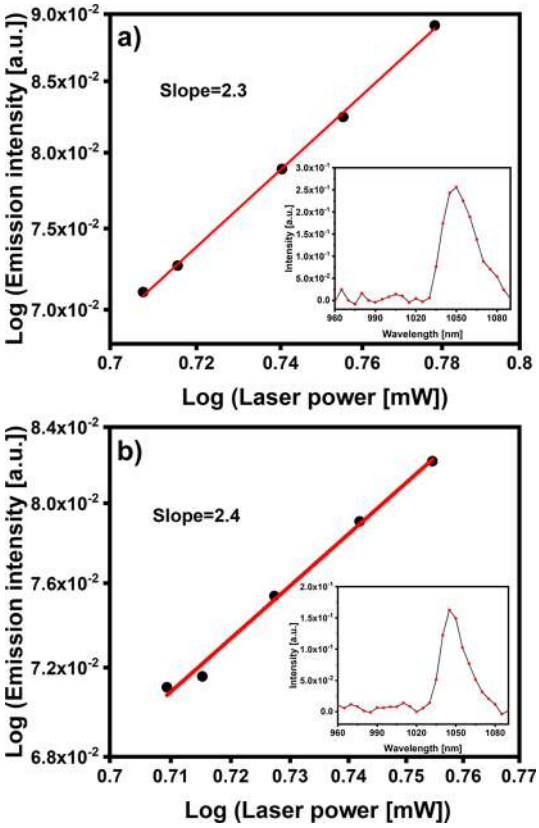

Figure 8. Dependency of the Nd^{3+} emission intensity at 1050 nm as a function of the 865 nm excitation average power in log−log plots for: (a) IR-phenNd(DBM)$_3$ and (b) IR-tpyNd(DBM)$_3$ (black symbols). The red lines indicate linear fits to the data. The respective baseline-corrected emission spectra of the antennas of Nd^{3+} complexes upon 865 nm femtosecond excitation are included in the insets (black lines with red symbols).

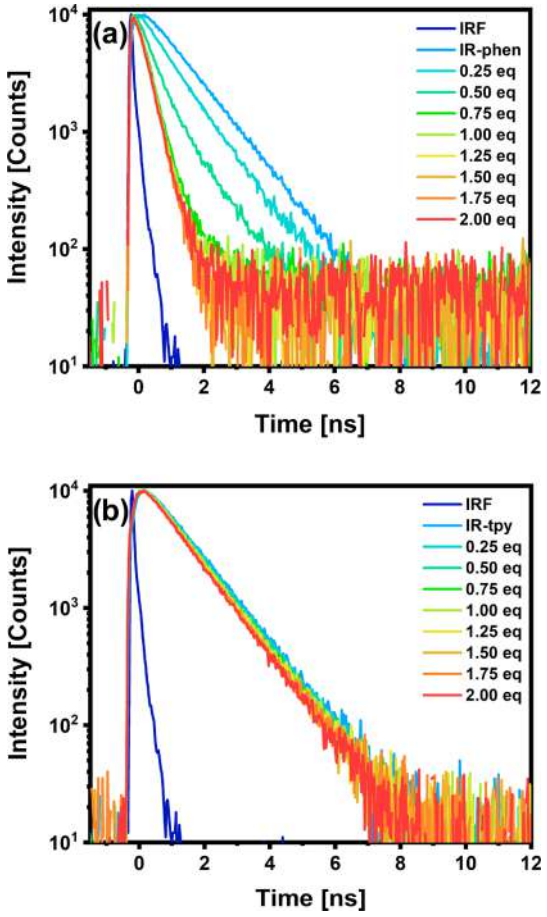

Figure 9. TCSPC traces after the addition of up to 2.0 equiv of Nd(DBM)$_3$(H$_2$O)$_2$. (a) for the IR-phen ligand and (b) for the IR-tpy ligand (colored continuous lines as indicated). The measurements were conducted in acetone at room temperature.

fluorometric titrations on 1.5 mL of 220 μM solutions of the ligands with additions of up to 2.0 equiv of Nd(DBM)$_3$(H$_2$O)$_2$ in 65 μL aliquots with 0.25 equiv each. As shown in Figure 9, when the ligand solutions are combined with the Nd(DBM)$_3$(H$_2$O)$_2$ aliquots, there are notable decreases in the ligand S_1 decay times, which are related with the formation of IR-phenNd(DBM)$_3$ and IR-tpyNd(DBM)$_3$ complexes. The most notable decrease in the S_1 lifetime corresponds to the IR-phen ligand, which goes from 1.2 ns to 300 ps. This corresponds to an energy transfer rate of 2.5×10^9 s^{-1} and a yield of 75%. On the other hand, for the IR-tpyNd(DBM)$_3$ case, the transfer rate corresponds to 1.4×10^8 s^{-1} and an efficiency of 15.4%.

The clear difference in energy transfer rates between IR-tpyNd(DBM)$_3$ and IR-phenNd(DBM)$_3$ can be directly related to the differences in their donor−acceptor distances. These distances were estimated from models using the optimized ligand geometries (see Computational Methods section) and typical distances between the Nd^{3+} center and the ligand nitrogen atoms of 2.6 Å.[10] For the IR-phenNd(DBM)$_3$ case, the distance from the polymethine meso carbon to the Nd^{3+} center corresponds to 7.9 Å, while for the IR-tpyNd(DBM)$_3$ case, this distance is longer due to the geometry of this ligand and the extra phenyl group, giving a value of 11.9 Å. A comparison of the experimental rates with a simple Förster model is included in a latter section.

As a control experiment, we performed the same titration using solutions of the IR-780 dye with the same addition of Nd(DBM)$_3$(H$_2$O)$_2$ aliquots. These solutions do not show any changes in the cyanine decay times (see Figure S15). Tables S1 and S2 summarize the fluorescence lifetimes, yields, and energy transfer rates observed for the polymethine ligands and Nd^{3+} complexes.

For our study, we considered it interesting to directly observe the formation of the complexes with the Nd^{3+} centers through their rotational diffusion properties, which can be directly measured through time resolution of the ligand emission anisotropies. The rotational diffusion of a molecule is commonly quantified by the time constant θ of an exponential fit to the fluorescence anisotropy decay trace $r(t)$

$$r(t) = \frac{I_{\parallel}(t) - I_{\perp}(t)}{I_{\parallel}(t) + 2I_{\perp}(t)}$$

where, $I_{\parallel}(t)$ is the time-dependent fluorescence intensity with polarization parallel to the excitation beam, and $I_{\perp}(t)$ is the respective intensity with perpendicular polarization. The θ values correspond to the molecular rotational relaxation times. The operating concept in these experiments is that, given the larger hydrodynamic volumes of Nd^{3+} complexes, slower rotational relaxation times, can be expected in comparison with the free ligands. A summary of the anisotropy results is included in Table S3, and the traces are shown in Figures S16−

https://doi.org/10.1021/acs.jpca.2c01052
J. Phys. Chem. A 2022, 126, 2498−2510

S19. The anisotropy traces of the Nd^{3+} complexes showed slower decays in comparison with the free ligands. The rotational relaxation times θ changed from 260 ± 29 to 355 ± 37 ps in going from IR-phen to IR-phenNd(DBM)$_3$, while for the terpyridine case, the θ values go from 222 ± 16 to 290 ± 30 ps. These increases in the rotational relaxation times are consistent with the presence of emitters with a larger hydrodynamic volume in IR-phenNd(DBM)$_3$ and IR-tpyNd-(DBM)$_3$ solutions in comparison with the ligand-only solutions, highlighting the formation of the complexes.

Energy Transfer Mechanism in Nd^{3+} Polymethinic Ligand Complexes. The energy transfer mechanism for the complexes is proposed considering the coincidence of the bands from the $^4F_{5/2} \leftarrow {}^4I_{9/2}$ transition of the Nd^{3+} ion with the lowest energy emission of the ligands, together with the decrease in the cyanine S_1 lifetimes, as shown in Figure 9. From these results, it can be concluded that the energy transfer takes place from the lowest-energy singlet state of the polymethine chain. Furthermore, these kinds of electronic transitions obey the Wigner−Witmer spin selection rules, which dictate that the total spin should not change during the transition.[92−95] The antenna multiplicity in the donor state is singlet, while the Nd^{3+} ion is has a quadruplet multiplicity, with a total spin $S = 3/2$. From the Wigner−Witmer rule, upon addition of the total spins $S_T = 0 + 3/2 = 3/2$, the spin is preserved at initial the final state of the transition. In addition to the spin conservation rules, transitions in lanthanide ions are governed by their own selection rules, which are derived from the Judd−Ofelt theory.[9,10,15]

From this theory, the following selection rules are derived: (a) $|\Delta J| = |J-J'| = 2, 4, 6$ and (b) $|\Delta J| = |J-J'| = 0, 1$ (for $J = J' = 0$, the transition is forbidden), where J and J' are the total angular momenta of the initial and final states, respectively. The $|\Delta J|$ can be associated with two canonical energy transfer mechanisms (multipolar and exchange mechanisms), where (a) corresponds to the Förster mechanism and (b) to the Dexter mechanism. Applying this selection rule for the observed transitions in the Nd^{3+} cyaninic complexes, $^4F_{3/2} \rightarrow {}^4I_{11/2}$, we have $|\Delta J| = |3/2-11/2| = 4$.[6,9,10,15,78] The energy migration in these complexes is then consistent with a through-space, Förster-type mechanism, which can be effective across distances of the order of a few nanometers. In the case of IR-phenNd(DBM)$_3$ and IR-tpyNd(DBM)$_3$, the center-to-center distances are 7.9 and 11.9 Å, respectively, which can be appropriate for a through-space type of mechanism as shown below.

The proposed series of steps for the sensitization upon simultaneous absorption of two photons is as follows: The antenna reaches the second excited state by two-photon absorption from the ground state: $S_2 \leftarrow S_0$; this is rapidly followed by internal conversion to form the S_1 fluorescent state, where this kind of emissive singlet is considered in the literature to have a small degree of intraligand charge transfer character.[96−102] Once this state is formed in the scale of a picosecond,[87] energy transfer can occur, forming the $^4F_{5/2}$ lanthanide state in kinetic competition with the radiative and nonradiative decay of the emissive cyanine state. After the energy migration step, conversion within the higher states of the Nd^{3+} ion occurs ($^4F_{5/2} \rightarrow {}^4F_{3/2}$). Finally, spontaneous emission from the metal center ($^4F_{3/2} \rightarrow {}^4I_{11/2}$) produces the band centered at 1050 nm. The energy transfer mechanism is summarized in Scheme 2.

Scheme 2. Energy Transfer Pathways for One- and Two-Photon Absorption (1PA and 2PA) in IR-phenNd(DBM)$_3$ and IR-tpyNd(DBM)$_3$[a]

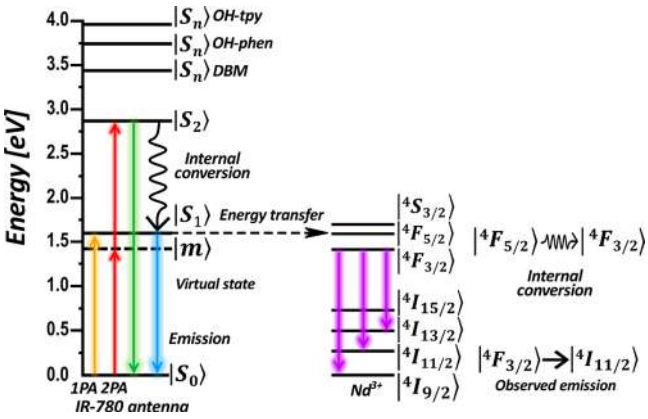

[a]According to this mechanism, the energy transfer occurs from the first locally excited singlet of the polymethine chain, toward the respective "receiver" excited state of the Nd^{3+} ion. In the case of simultaneous biphotonic sensitization with 865 nm pulses, the originally formed state is the second excited singlet in the cyanine antenna, a state with a large two-photon cross section.

The assignment of cyanine S_1 as donor states as opposed to the respective triplet states is actually consistent with studies by Chan, Cohen, Schuck, and co-workers who showed that the IR-806 cyanine, which has the exact same conjugation pattern as IR-780, has a T_1 energy of ≈1.25 eV.[103] This energy is below that required to promote a transition into the $^4F_{3/2}$ state, which lies 1.42 eV above the ion ground state.

To further support and highlight the participation of the S_1 cyanine state, the respective energy transfer efficiencies η_{et} were estimated considering a Förster-type model.[104] These calculations used the appropriate experimental parameters: the refractive index of acetone (1.357 at 800 nm), the IR-phen and IR-tpy fluorescence lifetimes (τ = 1.2 and 1.3 ns, respectively), the ligand S_1 emission quantum yields (0.31 and 0.36), the molar absorptivity of the $^4F_{5/2} \leftarrow {}^4I_{9/2}$ transition of the Nd^{3+} ion (ε = 3.6 M^{-1} cm^{-1} at λ = 800 nm), and finally, the distances between the polymethine antenna and the Nd^{3+} ion in both complexes from models built using the optimized ligand geometries and typical Nd^{3+} distances to the respective ligand atoms (2.6 Å).[10] In addition, following previous contributions, we considered a value of 2/3 as the isotropic limit of the orientation factor κ^2 for a dipolar-type interaction.[2,5] Using these parameters, the Förster model predicts an energy transfer efficiency of η_{et} = 99% for IR-phenNd(DBM)$_3$, and η_{et} = 63% for IR-tpyNd(DBM)$_3$. As can be seen, the Förster model overestimates the energy transfer efficiencies in comparison with the values obtained from the increase in the total S_1 decay rates shown in Figure 9. These differences are most likely related to the fact that the Förster model can severely overestimate the electronic couplings for distances of the order of 10 Å or less.[105−107] Such deviations arise from a failure of the point−dipole interaction assumed in the Förster model. These calculations, however, are consistent with the notion that the donor state in these cases corresponds to the first cyaninic excited singlet.

https://doi.org/10.1021/acs.jpca.2c01052
J. Phys. Chem. A 2022, 126, 2498−2510

CONCLUSIONS

In the present contribution, we aimed to demonstrate the possibility of a nonlinear optical scheme for sensitizing the emission of a lanthanide center through a polymethine antenna, where the electronic transitions were designed in a specific way with regard to the presence of an intermediate transition (near-resonant with the S_1 state of cyanine), a nonlinearly active state in the antenna (polymethinic S_2), and the respective energy alignment of the localized first singlet state of the ligand with an appropriate receiver state in the lanthanide ion. With this design, we synthesized two chromophoric ligands capable of coordinating the Nd^{3+} center, one based on a phenanthroline unit and the other on a phenyl-terpyridine unit. The full ligands have important two-photon absorption from the use of a polymethine chromophore derived from IR-780 cyanine directly bonded to the phenanthroline or phenyl-terpyridine units. We demonstrated the sensitization of the 1050 nm lanthanide emission of the respective Nd^{3+} complexes by NIR light upon one and simultaneous two-photon absorptions. Importantly, these complexes can be efficiently sensitized by regular linear excitation directly into the highly absorbing S_1 transition of the antenna with 780 nm light, a transition with one of the largest absorption coefficients of any chromophore.[108−120] The nonlinear optical excitation was achieved with 865 nm femtosecond pulses, which produces the emission of the Nd^{3+} ion, where the quadratic dependence typical of simultaneous two-photon absorption was verified. The nonlinear optical absorption is promoted by the S_2 and S_1 symmetries and an energy gap of 1.3 eV, which allows for a near-resonant step-like transition to the higher cyaninic state with a single-photon energy slightly below the first transition.[47,48,67,68] The energy transfer from the antenna chromophore to the Nd^{3+} ion occurs by a mechanism that is allowed by the Wigner−Witmer selection rules and by those derived from the Judd−Ofelt theory. The exciton migration most likely occurs through a Förster-type mechanism. Importantly, the phenanthroline-type ligand is approximately five times more efficient for the sensitization due to a shorter donor−acceptor distance in comparison with the phenyl-terpyridine ligand. This result indicates that the energy transfer step is highly sensitive to the distance of the Nd^{3+} center to the polymethinic ligand. Two-photon sensitization of lanthanide emission can have applications in areas that require high localization of the excitation events and long emission lifetimes, which in the case of Nd^{3+} have been observed to be in the range from 100 to 800 μs.[2,5,73,90,116,121,122]

ASSOCIATED CONTENT

Supporting Information

The Supporting Information is available free of charge at https://pubs.acs.org/doi/10.1021/acs.jpca.2c01052.

Synthesis procedures, spectroscopic characterization studies, static spectra of the components of the complexes, static spectra in acetone, experimental diagram for the two-photon excitation, time-resolved experiments, table of emission lifetimes during the fluorometric titrations, TCSPC results for the control experiments with IR-780 with added $Nd(DBM)_3(H_2O)_2$, table with total decay rates and energy transfer rates, table and graphs with time-resolved anisotropy results, computational chemistry results, calculation of energy transfer efficiencies under the Förster model, baseline treatment for the Nd^{3+} emission spectra, and coordinates of optimized geometries (PDF)

AUTHOR INFORMATION

Corresponding Author

Jorge Peón − *Instituto de Química, Universidad Nacional Autónoma de México, Ciudad de México 04510, México;* orcid.org/0000-0002-4571-5136; Email: jpeon@unam.mx

Authors

Jesús Durán-Hernández − *Instituto de Química, Universidad Nacional Autónoma de México, Ciudad de México 04510, México*

Leonardo Muñoz-Rugeles − *Instituto de Química, Universidad Nacional Autónoma de México, Ciudad de México 04510, México*

Óscar Guzmán-Méndez − *Instituto de Química, Universidad Nacional Autónoma de México, Ciudad de México 04510, México*

Mariana M Reza − *Instituto de Química, Universidad Nacional Autónoma de México, Ciudad de México 04510, México*

Andrea Cadena-Caicedo − *Instituto de Química, Universidad Nacional Autónoma de México, Ciudad de México 04510, México*

Verónica García-Montalvo − *Instituto de Química, Universidad Nacional Autónoma de México, Ciudad de México 04510, México;* orcid.org/0000-0002-6220-9702

Complete contact information is available at: https://pubs.acs.org/10.1021/acs.jpca.2c01052

Notes

The authors declare no competing financial interest.

ACKNOWLEDGMENTS

The authors acknowledge the CONACyT-México grant Ciencia de Frontera 2019-51496 and PAPIIT/DGAPA/UNAM IG200621 for financial support and DGTIC-UNAM project LANCAD-UNAM-DGTIC-210 for computer time. The authors thank Everardo Tapia Mendoza of the LANCIC Laboratory for mass spectrometry experiments.

REFERENCES

(1) Armelao, L.; Quici, S.; Barigelletti, F.; Accorsi, G.; Bottaro, G.; Cavazzini, M.; Tondello, E. Design of Luminescent Lanthanide Complexes: From Molecules to Highly Efficient Photo-Emitting Materials. *Coord. Chem. Rev.* **2010**, *254*, 487−505.

(2) Bünzli, J. G.; Piguet, C. Taking Advantage of Luminescent Lanthanide Ions. *Chem. Soc. Rev.* **2005**, *34*, 1048−1077.

(3) D'Aléo, A.; Pompidor, G.; Elena, B.; Vicat, J.; Baldeck, P. L.; Toupet, L.; Kahn, R.; Andraud, C.; Maury, O. Two-Photon Microscopy and Spectroscopy of Lanthanide Bioprobes. *ChemPhysChem* **2007**, *8*, 2125−2132.

(4) Sousa Filho, P. C. d.; Lima, J. F.; Serra, O. A. From Lighting to Photoprotection: Fundamentals and Applications of Rare Earth Materials. *J. Braz. Chem. Soc.* **2015**, *26*, 2471−2495.

(5) Bünzli, J. G. Lanthanide Luminescence for Biomedical Analyses and Imaging. *Chem. Rev.* **2010**, *110*, 2729−2755.

(6) Eliseeva, S.; Bünzli, J. C. G. Lanthanide Luminescence for Functional Materials and Bio-Sciences. *Chem. Soc. Rev.* **2010**, *39*, 189−227.

(7) Law, G. L.; Wong, K. L.; Man, C. W. Y.; Tsao, S. W.; Wong, W. T. A Two-Photon Europium Complex as Specific Endoplasmic Reticulum Probe. *J. Biophotonics* **2009**, *2*, 718−724.
(8) Zhang, K. Y.; Yu, Q.; Wei, H.; Liu, S.; Zhao, Q.; Huang, W. Long-Lived Emissive Probes for Time-Resolved Photoluminescence Bioimaging and Biosensing. *Chem. Rev.* **2018**, *118*, 1770−1839.
(9) *Luminescence of Lanthanide Ions in Coordination Compounds and Nanomaterials*; de Bettencourt-Dias, A., Ed.; Wiley: University of Nevada: Reno, USA, 2014.
(10) *Rare Earth Coordination Chemistry. Fundamentals and Applications*; Huang, C.-H., Ed.; Wiley: Peking University: China, 2010.
(11) *Spectroscopic Properties of Rare Earths in Optical Materials*; Guokui, L.; Bernard, J., Eds.; Tsinghua University Press: Pekin, China, 2005.
(12) Dexter, D. L. A Theory of Sensitized Luminescence in Solids. *J. Chem. Phys.* **1953**, *21*, 836−850.
(13) Faustino, W. M.; Malta, O. L.; de Sá, G. F. Intramolecular Energy Transfer through Charge Transfer State in Lanthanide Compounds: A Theoretical Approach. *J. Chem. Phys.* **2005**, *122*, No. 054109.
(14) Főrster, T. 10th Spiers Memorial Lecture. Transfer Mechanisms of Electronic Excitation. *Discuss. Faraday Soc.* **1959**, *27*, 7−17.
(15) Malta, O. L. Ligand—Rare-Earth Ion Energy Transfer in Coordination Compounds. A Theoretical Approach. *J. Lumin.* **1997**, *71*, 229−236.
(16) Olaya-Castro, A.; Scholes, G. D. Energy Transfer from Förster-Dexter Theory to Quantum Coherent Light-Harvesting. *Int. Rev. Phys. Chem.* **2011**, *30*, 49−77.
(17) e Silva, F. R.; Malta, O. L. Calculation of the Ligand-Lanthanide Ion Energy Transfer Rate in Coordination Compounds: Contributions of Exchange Interactions. *J. Alloys Compd.* **1997**, *250*, 427−430.
(18) Guzmán-Méndez, Ó.; González, F.; Bernès, S.; Flores-Álamo, M.; Ordóñez-Hernández, J.; García-Ortega, H.; Guerrero, J.; Qian, W.; Aliaga-Alcalde, N.; Gasque, L. Coumarin Derivative Directly Coordinated to Lanthanides Acts as an Excellent Antenna for UV-Vis and Near-IR Emission. *Inorg. Chem.* **2018**, *57*, 908−911.
(19) Correa-Ascencio, M.; Galván-Miranda, E. K.; Rascón-Cruz, F.; Jiménez-Sandoval, O.; Jiménez-Sandoval, S. J.; Cea-Olivares, R.; Jancik, V.; Toscano, R. A.; García-Montalvo, V. Lanthanide(III) Complexes with 4,5-Bis(Diphenylphosphinoyl)-1,2,3- Triazolate and the Use of 1,10-Phenanthroline as Auxiliary Ligand. *Inorg. Chem.* **2010**, *49*, 4109−4116.
(20) Meshkova, S. B. The Dependence of the Luminescence Intensity of Lanthanide Complexes with β-Diketones on the Ligand Form. *J. Fluoresc.* **2000**, *10*, 333−338.
(21) Ferreira Da Rosa, P. P.; Miyazaki, S.; Sakamoto, H.; Kitagawa, Y.; Miyata, K.; Akama, T.; Kobayashi, M.; Fushimi, K.; Onda, K.; Taketsugu, T.; et al. Coordination Geometrical Effect on Ligand-to-Metal Charge Transfer-Dependent Energy Transfer Processes of Luminescent Eu(III) Complexes. *J. Phys. Chem. A* **2021**, *125*, 209−217.
(22) Andres, J.; Chauvin, A. S. Energy Transfer in Coumarin-Sensitised Lanthanide Luminescence: Investigation of the Nature of the Sensitiser and Its Distance to the Lanthanide Ion. *Phys. Chem. Chem. Phys.* **2013**, *15*, 15981−15994.
(23) Delaey, E.; van Laar, F.; De Vos, D.; Kamuhabwa, A.; Jacobs, P.; de Witte, P. A Comparative Study of the Photosensitizing Characteristics of Some Cyanine Dyes. *J. Photochem. Photobiol., B* **2000**, *55*, 27−36.
(24) Le Guennic, B.; Jacquemin, D. Taking Up the Cyanine Challenge with Quantum Tools. *Acc. Chem. Res.* **2015**, *48*, 530−537.
(25) Mishra, A.; Behera, R. K.; Behera, P. K.; Mishra, B. K.; Behera, G. B. Cyanines during the 1990s: A Review. *Chem. Rev.* **2000**, *100*, 1973−2011.
(26) Mustroph, H.; Reiner, K.; Mistol, J.; Ernst, S.; Keil, D.; Hennig, L. Relationship between the Molecular Structure of Cyanine Dyes and the Vibrational Fine Structure of Their Electronic Absorption Spectra. *ChemPhysChem* **2009**, *10*, 835−840.
(27) Belfield, K. D.; Bondar, M. V.; Hernandez, F. E.; Przhonska, O.; Yao, S. Two-Photon Absorption of a Supramolecular Pseudoisocyanine J-Aggregate Assembly. *Chem. Phys.* **2006**, *320*, 118−124.
(28) El-Shishtawy, R. M.; Al-Zahrani, F. A. M.; Afzal, S. M.; Razvi, M. A. N.; Al-Amshany, Z. M.; Bakry, A. H.; Asiri, A. M. Synthesis, Linear and Nonlinear Optical Properties of a New Dimethine Cyanine Dye Derived from Phenothiazine. *RSC Adv.* **2016**, *6*, 91546−91556.
(29) Fu, J.; Padilha, L. A.; Hagan, D. J.; van Stryland, E. W.; Przhonska, O. V.; Bondar, M. V.; Slominsky, Y. L.; Kachkovski, A. D. Experimental and Theoretical Approaches to Understanding Two-Photon Absorption Spectra in Polymethine and Squaraine Molecules. *J. Opt. Soc. Am. B* **2007**, *24*, No. 67.
(30) Kwok, S. J. J.; Choi, M.; Bhayana, B.; Zhang, X.; Ran, C.; Yun, S. H. Two-Photon Excited Photoconversion of Cyanine-Based Dyes. *Sci. Rep.* **2016**, *6*, No. 23866.
(31) Padilha, L. A.; Webster, S.; Przhonska, O. V.; Hu, H.; Peceli, D.; Rosch, J. L.; Bondar, M. V.; Gerasov, A. O.; Kovtun, Y. P.; Shandura, M. P.; et al. Nonlinear Absorption in a Series of Donor-π-Acceptor Cyanines with Different Conjugation Lengths. *J. Mater. Chem.* **2009**, *19*, 7503−7513.
(32) Sun, R.; Yan, B. L.; Ge, J. F.; Xu, Q. F.; Li, N. J.; Wu, X. Z.; Song, Y. L.; Lu, J. M. Third-Order Nonlinear Optical Properties of Unsymmetric Pentamethine Cyanine Dyes Possessing Benzoxazolyl and Benzothiazolyl Groups. *Dyes Pigm.* **2013**, *96*, 189−195.
(33) Feng, L.; Chen, W.; Ma, X.; Liu, S. H.; Yin, J. Near-Infrared Heptamethine Cyanines (Cy7): From Structure, Property to Application. *Org. Biomol. Chem.* **2020**, *18*, 9385−9397.
(34) Gorka, A. P.; Nani, R. R.; Schnermann, M. J. Harnessing Cyanine Reactivity for Optical Imaging and Drug Delivery. *Acc. Chem. Res.* **2018**, *51*, 3226−3235.
(35) Li, M.; Sun, W.; Tian, R.; Cao, J.; Tian, Y.; Gurram, B.; Fan, J.; Peng, X. Smart J-Aggregate of Cyanine Photosensitizer with the Ability to Target Tumor and Enhance Photodynamic Therapy Efficacy. *Biomaterials* **2021**, *269*, No. 120532.
(36) Poplinger, D.; Bazylevich, A.; Bokan, M.; Gellerman, G.; Patsenker, L. Dual-Dye Systems Comprising Activatable Fluorescein Dye and Hydrophobic or Hydrophilic Cy5 Reference Fluorophore for Ratiometric Drug Delivery Monitoring. *J. Photochem. Photobiol., A* **2021**, *408*, No. 113113.
(37) Siriwibool, S.; Kaekratoke, N.; Chansaenpak, K.; Siwawannapong, K.; Panajapo, P.; Sagarik, K.; Noisa, P.; Lai, R. Y.; Kamkaew, A. Near-Infrared Fluorescent PH Responsive Probe for Targeted Photodynamic Cancer Therapy. *Sci. Rep.* **2020**, *10*, No. 1283.
(38) Xu, Z.; Huang, X.; Zhang, M. X.; Chen, W.; Liu, S. H.; Tan, Y.; Yin, J. Tissue Imaging of Glutathione-Specific Naphthalimide-Cyanine Dye with Two-Photon and Near-Infrared Manners. *Anal. Chem.* **2019**, *91*, 11343−11348.
(39) Bao, G.; Wen, S.; Lin, G.; Yuan, J.; Lin, J.; Wong, K. L.; Bünzli, J. C. G.; Jin, D. Learning from Lanthanide Complexes: The Development of Dye-Lanthanide Nanoparticles and Their Biomedical Applications. *Coord. Chem. Rev.* **2021**, *429*, No. 213642.
(40) Han, S.; Deng, R.; Xie, X.; Liu, X. Enhancing Luminescence in Lanthanide-Doped Upconversion Nanoparticles. *Angew. Chem., Int. Ed.* **2014**, *53*, 11702−11715.
(41) Wang, X.; Valiev, R. R.; Ohulchanskyy, T. Y.; Ågren, H.; Yang, C.; Chen, G. Dye-Sensitized Lanthanide-Doped Upconversion Nanoparticles. *Chem. Soc. Rev.* **2017**, *46*, 4150−4167.
(42) Wang, S.; Wang, L. Lanthanide-Doped Nanomaterials for Luminescence Detection and Imaging. *TrAC, Trends Anal. Chem.* **2014**, *62*, 123−134.
(43) Wei, W.; Chen, G.; Baev, A.; He, G. S.; Shao, W.; Damasco, J.; Prasad, P. N. Alleviating Luminescence Concentration Quenching in Upconversion Nanoparticles through Organic Dye Sensitization. *J. Am. Chem. Soc.* **2016**, *138*, 15130−15133.

https://doi.org/10.1021/acs.jpca.2c01052
J. Phys. Chem. A 2022, 126, 2498−2510

(44) Xie, X.; Li, Z.; Zhang, Y.; Guo, S.; Pendharkar, A. I.; Lu, M.; Huang, L.; Huang, W.; Han, G. Emerging ≈800 Nm Excited Lanthanide-Doped Upconversion Nanoparticles. *Small* **2017**, *13*, No. 1602843.
(45) Pascal, S.; Haefele, A.; Monnereau, C.; Charaf-Eddin, A.; Jacquemin, D.; le Guennic, B.; Andraud, C.; Maury, O. Expanding the Polymethine Paradigm: Evidence for the Contribution of a Bis-Dipolar Electronic Structure. *J. Phys. Chem. A* **2014**, *118*, 4038−4047.
(46) Levitz, A.; Marmarchi, F.; Henary, M. Synthesis and Optical Properties of Near-Infrared Meso-Phenyl-Substituted Symmetric Heptamethine Cyanine Dyes. *Molecules* **2018**, *23*, No. 226.
(47) Villatoro, E.; Muñoz-Rugeles, L.; Durán-Hernández, J.; Salcido-Santacruz, B.; Esturau-Escofet, N.; López-Cortés, J. G.; Ortega-Alfaro, M. C.; Peón, J. Two-Photon Induced Isomerization through a Cyaninic Molecular Antenna in Azo Compounds. *Chem. Commun.* **2021**, *57*, 3123−3126.
(48) Rodríguez-Romero, J.; Guarin, C. A.; Arroyo-Pieck, A.; Gutiérrez-Arzaluz, L.; López-Arteaga, R.; Cortés-Guzmán, F.; Navarro, P.; Peon, J. Fluorophore Release from a Polymethinic Photoremovable Protecting Group Through a Nonlinear Optical Process. *ChemPhotoChem* **2017**, *1*, 397−407.
(49) Arroyo-Pieck, A.; Araiza-Olivera, D.; Peon, J. Bichromophoric Sensors for Ratiometric Measurements of Molecular Microenvironments through the Interplay of Charge Transfer and Energy Transfer Channels. *ChemPlusChem* **2018**, *83*, 1097−1108.
(50) Guo, L.; Chan, M. S.; Xu, D.; Tam, D. Y.; Bolze, F.; Lo, P. K.; Wong, M. S. Indole-Based Cyanine as a Nuclear RNA-Selective Two-Photon Fluorescent Probe for Live Cell Imaging. *ACS Chem. Biol.* **2015**, *10*, 1171−1175.
(51) Juvekar, V.; Lim, C. S.; Lee, D. J.; Park, S. J.; Song, G. O.; Kang, H.; Kim, H. M. An Azo Dye for Photodynamic Therapy That Is Activated Selectively by Two-Photon Excitation. *Chem. Sci.* **2021**, *12*, 427−434.
(52) Ohulchanskyy, T. Y.; Pudavar, H. E.; Yarmoluk, S. M.; Yashchuk, V. M.; Bergey, E. J.; Prasad, P. N. A Monomethine Cyanine Dye Cyan 40 for Two-Photon−Excited Fluorescence Detection of Nucleic Acids and Their Visualization in Live Cells. *Photochem. Photobiol.* **2003**, *77*, 138−145.
(53) Park, H. J.; Song, C. W.; Sarkar, S.; Jun, Y. W.; Reo, Y. J.; Dai, M.; Ahn, K. H. A Caveat to Common Hemicyanine Dye Components and Their Resolution. *Chem. Commun.* **2020**, *56*, 7025−7028.
(54) Velema, W. A.; Szymanski, W.; Feringa, B. L. Photopharmacology: Beyond Proof of Principle. *J. Am. Chem. Soc.* **2014**, *136*, 2178−2191.
(55) Yang, W.; Shan Chan, P.; Shan Chan, M.; Fai Li, K.; Kwan Lo, P.; Ki Mak, N.; Wai Cheah, K.; Shing Wong, M. Two-Photon Fluorescence Probes for Imaging of Mitochondria and Lysosomes. *Chem. Commun.* **2013**, *49*, 3428−3430.
(56) Brown, E. B.; Shear, J. B.; Adams, S. R.; Tsien, R. Y.; Webb, W. W. Photolysis of Caged Calcium in Femtoliter Volumes Using Two-Photon Excitation. *Biophys. J.* **1999**, *76*, 489−499.
(57) Chiu, D. T.; Lorenz, R. M.; Jeffries, G. D. M. Droplets for Ultrasmall-Volume Analysis. *Anal. Chem.* **2009**, *81*, 5111−5118.
(58) Diaspro, A.; Bianchini, P.; Vicidomini, G.; Faretta, M.; Ramoino, P.; Usai, C. Multi-Photon Excitation Microscopy. *Biomed. Eng. Online* **2006**, *5*, No. 36.
(59) Zipfel, W. R.; Williams, R. M.; Webb, W. W. Nonlinear Magic: Multiphoton Microscopy in the Biosciences. *Nat. Biotechnol.* **2003**, *21*, 1369−1377.
(60) Qi, J.; Sun, C.; Li, D.; Zhang, H.; Yu, W.; Zebibula, A.; Lam, J. W. Y.; Xi, W.; Zhu, L.; Cai, F.; et al. Aggregation-Induced Emission Luminogen with near-Infrared-II Excitation and near-Infrared-I Emission for Ultradeep Intravital Two-Photon Microscopy. *ACS Nano* **2018**, *12*, 7936−7945.
(61) Zhuang, W.; Yang, L.; Ma, B.; Kong, Q.; Li, G.; Wang, Y.; Tang, B. Z. Multifunctional Two-Photon AIE Luminogens for Highly Mitochondria-Specific Bioimaging and Efficient Photodynamic Therapy. *ACS Appl. Mater. Interfaces* **2019**, *11*, 20715−20724.
(62) Wang, S.; Chen, H.; Liu, J.; Chen, C.; Liu, B. NIR-II Light Activated Photosensitizer with Aggregation-Induced Emission for Precise and Efficient Two-Photon Photodynamic Cancer Cell Ablation. *Adv. Funct. Mater.* **2020**, *30*, No. 2002546.
(63) Cabral Campello, M. P.; Palma, E.; Correia, I.; Paulo, P. M. R.; Matos, A.; Rino, J.; Coimbra, J.; Pessoa, J. C.; Gambino, D.; Paulo, A.; et al. Lanthanide Complexes with Phenanthroline-Based Ligands: Insights into Cell Death Mechanisms Obtained by Microscopy Techniques. *Dalton Trans.* **2019**, *48*, 4611−4624.
(64) Cai, L. L.; Hu, Y. T.; Li, Y.; Wang, K.; Zhang, X. Q.; Muller, G.; Li, X. M.; Wang, G. X. Solid-State Luminescence Properties, Hirshfeld Surface Analysis and DFT Calculations of Mononuclear Lanthanide Complexes (Ln = Eu^{III}, Gd^{III}, Tb^{III}, Dy^{III}) Containing 4′-Phenyl-2,2′:6′,2″-Terpyridine. *Inorg. Chim. Acta* **2019**, *489*, 85−92.
(65) Wong, H. Y.; Lo, W. S.; Chan, W. T. K.; Law, G. L. Mechanistic Investigation of Inducing Triboluminescence in Lanthanide(III) β-Diketonate Complexes. *Inorg. Chem.* **2017**, *56*, 5135−5140.
(66) Ying-Ying, L.; Ning, R.; Shu-Ping, W.; Jian-Jun, Z. A Series of Lanthanide Complexes with 2,4-Dimethylbenzoic Acid and 2,2:6′,2″-Terpyridine: Supramolecular Structures, Thermal Decomposition Mechanism and Photoluminescence. *Inorg. Chim. Acta* **2020**, *510*, No. 119755.
(67) Guarin, C. A.; Mendoza-Luna, L. G.; Haro-Poniatowski, E.; Hernández-Pozos, J. L. Two-Photon Absorption Spectrum and Characterization of the Upper Electronic States of the Dye IR780. *Spectrochim. Acta, Part A* **2021**, *249*, No. 119291.
(68) Mendoza-Luna, L. G.; Guarin, C. A.; Haro-Poniatowski, E.; Hernández-Pozos, J. L. Experimental and Computational Data on Two-Photon Absorption and Spectral Deconvolution of the Upper Excited States of Dye IR780. *Data Brief* **2021**, *35*, No. 106752.
(69) Durán-Hernández, J.; Muñoz-Rugeles, L.; Peón-Peralta, J. In *Sensitization Near-Infrared Luminescence of Nd(III) by Two-Photon Absorption of IR-780 Dye Functionalized with Phenanthroline and Terpyridine Derivatives*, Presented at Química y Materiales en el Siglo XIX. Future of Science 2019 México; Berkeley Global Science Institute: CDMX, México, 2019.
(70) Fu, L. M.; Wen, X. F.; Ai, X. C.; Sun, Y.; Wu, Y. S.; Zhang, J. P.; Wang, Y. Efficient Two-Photon-Sensitized Luminescence of a Europium(III) Complex. *Angew. Chem., Int. Ed.* **2005**, *44*, 747−750.
(71) Hao, R.; Li, M.; Wang, Y.; Zhang, J.; Ma, Y.; Fu, L.; Wen, X.; Wu, Y.; Ai, X.; Zhang, S.; et al. A Europium Complex with Excellent Two-Photon-Sensitized Luminescence Properties. *Adv. Funct. Mater.* **2007**, *17*, 3663−3669.
(72) Hebbink, G. A.; Klink, S. I.; Grave, L.; Oude Alink, P. G. B.; Van Veggel, F. C. J. M. Singlet Energy Transfer as the Main Pathway in the Sensitization of Near-Infrared Nd3+ Luminescence by Dansyl and Lissamine Dyes. *ChemPhysChem* **2002**, *3*, 1014−1018.
(73) Klink, S. I.; Grave, L.; Reinhoudt, D. N.; Van Veggel, F. C. J. M.; Werts, M. H. V.; Geurts, F. A. J.; Hofstraat, J. W. A Systematic Study of the Photophysical Processes in Polydentate Triphenylene-Functionalized Eu^{3+}, Tb^{3+}, Nd^{3+}, Yb^{3+}, and Er^{3+} Complexes. *J. Phys. Chem. A* **2000**, *104*, 5457−5468.
(74) Mironov, L. Y.; Sveshnikova, E. B.; Ermolaev, V. L. Energy Transfer from the Singlet Levels of Diketones and Dyes to Lanthanide Ions in Nanoparticles Consisting of Their Diketonate Complexes. *Opt. Spectrosc.* **2014**, *116*, 933−940.
(75) Yang, C.; Fu, L. M.; Wang, Y.; Zhang, J. P.; Wong, W. T.; Ai, X. C.; Qiao, Y. F.; Zou, B. S.; Gui, L. L. A Highly Luminescent Europium Complex Showing Visible-Light-Sensitized Red Emission: Direct Observation of the Singlet Pathway. *Angew. Chem., Int. Ed.* **2004**, *43*, 5010−5013.
(76) Golesorkhi, B.; Naseri, S.; Guénée, L.; Taarit, I.; Alves, F.; Nozary, H.; Piguet, C. Ligand-Sensitized Near-Infrared to Visible Linear Light Upconversion in a Discrete Molecular Erbium Complex. *J. Am. Chem. Soc.* **2021**, *143*, 15326−15334.
(77) Hyppänen, I.; Lahtinen, S.; Ääritalo, T.; Mäkelä, J.; Kankare, J.; Soukka, T. Photon Upconversion in a Molecular Lanthanide Complex in Anhydrous Solution at Room Temperature. *ACS Photonics* **2014**, *1*, 394−397.

https://doi.org/10.1021/acs.jpca.2c01052
J. Phys. Chem. A 2022, 126, 2498−2510

(78) Wang, H.; Yang, Y.; Cui, Y.; Wang, Z.; Qian, G. Sensitized Near-Infrared Luminescence from Erbium Ion-Associated Complex with IR140 Dye. *Dyes Pigm.* **2012**, *95*, 69−73.
(79) Liu, M.; Jia, M.; Pan, H.; Li, L.; Chang, M.; Ren, H.; Argoul, F.; Zhang, S.; Xu, J. Instrument Response Standard in Time-Resolved Fluorescence Spectroscopy at Visible Wavelength: Quenched Fluorescein Sodium. *Appl. Spectrosc.* **2014**, *68*, 577−583.
(80) Howell, B. A.; Dumitrascu, A. Thermal Stability of Bidendate Nitrogen Ligands Tethered to Multiwall Carbon Nanotubes. *J. Therm. Anal. Calorim.* **2010**, *102*, 505−512.
(81) Slough, G. A.; Krchňák, V.; Helquist, P.; Canham, S. M. Synthesis of Readily Cleavable Immobilized 1,10-Phenanthroline Resins. *Org. Lett.* **2004**, *6*, 2909−2912.
(82) Bao, X.; Liu, J.; Zheng, Q.; Pei, W.; Yang, Y.; Dai, Y.; Tu, T. Visual Recognition of Melamine in Milk via Selective Metallo-Hydrogel Formation. *Chin. Chem. Lett.* **2019**, *30*, 2266−2270.
(83) Oyetade, O. A.; Nyamori, V. O.; Martincigh, B. S.; Jonnalagadda, S. B. Nitrogen-Functionalised Carbon Nanotubes as a Novel Adsorbent for the Removal of Cu(II) from Aqueous Solution. *RSC Adv.* **2016**, *6*, 2731−2745.
(84) Li, W.; Li, J.; Li, H.; Yan, P.; Hou, G.; Li, G. NIR Luminescence of 2-(2,2,2-Trifluoroethyl)-1-Indone (TFI) Neodymium and Ytterbium Complexes. *J. Lumin.* **2014**, *146*, 205−210.
(85) Stanley, J. M.; Chan, C. K.; Yang, X.; Jones, R. A.; Holliday, B. J. Synthesis, X-Ray Crystal Structure and Photophysical Properties of Tris(Dibenzoylmethanido)(1,10-Phenanthroline)Samarium(III). *Polyhedron* **2010**, *29*, 2511−2515.
(86) Frisch, M. J.; Trucks, G. W.; Schlegel, H. B.; Scuseria, G. E.; Robb, M. A.; Cheeseman, J. R.; Scalmani, G.; Barone, V.; Petersson, G. A.; Nakatsuji, H.; et al. *Gaussian 16*, revision A.03; Gaussian, Inc.: Wallingford, CT, 2016.
(87) Guarin, C. A.; Villabona-Monsalve, J. P.; López-Arteaga, R.; Peon, J. Dynamics of the Higher Lying Excited States of Cyanine Dyes. An Ultrafast Fluorescence Study. *J. Phys. Chem. B* **2013**, *117*, 7352−7362.
(88) Crosby, G. A.; Kasha, M. Lntramofecular Energy Transfer in Ytterbium Orgmic CheIatest. *Spectrochim. Acta* **1958**, *10*, 377−382.
(89) Beeby, A.; Faulkner, S. Luminescence from Neodymium(III) in Solution. *Chem. Phys. Lett.* **1997**, *266*, 116−122.
(90) Hasegawa, Y.; Ohkubo, T.; Sogabe, K.; Kawamura, Y.; Wada, Y.; Nakashima, N.; Yanagida, S. Luminescence of Novel Neodymium Sulfonylaminate Complexes in Organic Media. *Angew. Chem., Int. Ed.* **2000**, *39*, 357−360.
(91) Uh, H.; Badger, P. D.; Geib, S. J.; Petoud, S. Synthesis and Solid-State, Solution, and Luminescence Properties of near-Infrared-Emitting Neodymium(3+) Complexes Formed with Ligands Derived from Salophen. *Helv. Chim. Acta* **2009**, *92*, 2313−2329.
(92) Bellary, V. P.; Balasubramanian, T. K.; Shetty, B. J. On the Wigner-Witmer Correlation Rules for a Homonuclear Diatomic Molecule with the like Atoms in Identical Atomic States. *Pramana* **1998**, *51*, 445−452.
(93) Persico, M.; Granucci, G. *Photochemistry: A Modern Theoretical Perspective*; Springer, 2018.
(94) Chiu, Y. N. Reformulation and Extension of Wigner-Witmer and Mulliken's Correlation Rules for the Spin and Orbital States of Diatomic Molecules upon Dissociation. *J. Chem. Phys.* **1973**, *58*, 722−726.
(95) Yamakawa, K.; Fukutani, K. Derivation of the Wigner-Witmer Rules in Terms of N-Electron Exchange. *J. Phys. B* **2013**, *46*, No. 085101.
(96) Zhou, L. C.; Zhao, G. J.; Liu, J. F.; Han, K. L.; Wu, Y. K.; Peng, X. J.; Sun, M. T. The Charge Transfer Mechanism and Spectral Properties of a Near-Infrared Heptamethine Cyanine Dye in Alcoholic and Aprotic Solvents. *J. Photochem. Photobiol., A* **2007**, *187*, 305−310.
(97) Zhou, L. C.; Liu, J. Y.; Zhao, G. J.; Shi, Y.; Peng, X. J.; Han, K. L. The Ultrafast Dynamics of Near-Infrared Heptamethine Cyanine Dye in Alcoholic and Aprotic Solvents. *Chem. Phys.* **2007**, *333*, 179−185.
(98) Wu, X. L.; Heikal, A. A.; Lee, I. Y. S.; Bohorquez, M.; Perry, J. W. Photoinduced Intermolecular Charge-Transfer Systems for Optical Limiting. *Mater. Res. Soc. Symp. Proc.* **1997**, *479*, 103−110.
(99) Peng, X.; Song, F.; Lu, E.; Wang, Y.; Zhou, W.; Fan, J.; Gao, Y. Heptamethine Cyanine Dyes with a Large Stokes Shift and Strong Fluorescence: A Paradigm for Excited-State Intramolecular Charge Transfer. *J. Am. Chem. Soc.* **2005**, *127*, 4170−4171.
(100) Grabowski, Z. R.; Rotkiewicz, K.; Rettig, W. Structural Changes Accompanying Intramolecular Electron Transfer: Focus on Twisted Intramolecular Charge-Transfer States and Structures. *Chem. Rev.* **2003**, *103*, 3899−4031.
(101) Kumar Das, D.; Makhal, K.; Goswami, D. Observing Ground State Vibrational Coherence and Excited State Relaxation Dynamics of a Cyanine Dye in Pure Solvents. *Phys. Chem. Chem. Phys.* **2018**, *20*, 13400−13411.
(102) Lutsyk, P.; Piryatinski, Y.; Kachkovsky, O.; Verbitsky, A.; Rozhin, A. Unsymmetrical Relaxation Paths of the Excited States in Cyanine Dyes Detected by Time-Resolved Fluorescence: Polymethinic and Polyenic Forms. *J. Phys. Chem. A* **2017**, *121*, 8236−8246.
(103) Garfield, D. J.; Borys, N. J.; Hamed, S. M.; Torquato, N. A.; Tajon, C. A.; Tian, B.; Shevitski, B.; Barnard, E. S.; Suh, Y. D.; Aloni, S.; et al. Enrichment of Molecular Antenna Triplets Amplifies Upconverting Nanoparticle Emission. *Nat. Photonics* **2018**, *12*, 402−407.
(104) Taniguchi, M.; Du, H.; Lindsey, J. S. PhotochemCAD 3: Diverse Modules for Photophysical Calculations with Multiple Spectral Databases. *Photochem. Photobiol.* **2018**, *94*, 277−289.
(105) Sobakinskaya, E.; Schmidt am Busch, M.; Renger, T. Theory of FRET "Spectroscopic Ruler" for Short Distances: Application to Polyproline. *J. Phys. Chem. B* **2018**, *122*, 54−67.
(106) Wong, K. F.; Bagchi, B.; Rossky, P. J. Distance and Orientation Dependence of Excitation Transfer Rates in Conjugated Systems: Beyond the Förster Theory. *J. Phys. Chem. A* **2004**, *108*, 5752−5763.
(107) Krueger, B. P.; Scholes, G. D.; Fleming, G. R. Calculation of Couplings and Energy-Transfer Pathways between the Pigments of LH2 by the Ab Initio Transition Density Cube Method. *J. Phys. Chem. A* **1998**, *102*, 5378−5386.
(108) Chapman, G.; Henary, M.; Patonay, G. The Effect of Varying Short-Chain Alkyl Substitution on the Molar Absorptivity and Quantum Yield of Cyanine Dyes. *Anal. Chem. Insights* **2011**, *6*, 29−36.
(109) Ahmed, Z.; Iftikhar, K. Sensitization of Visible and NIR Emitting Lanthanide(III) Ions in Noncentrosymmetric Complexes of Hexafluoroacetylacetone and Unsubstituted Monodentate Pyrazole. *J. Phys. Chem. A* **2013**, *117*, 11183−11201.
(110) Iwamuro, M.; Wada, Y.; Kitamura, T.; Nakashima, N.; et al. Photosensitized Luminescence of Novel β-Diketonato Nd(III) complexes in solution. *Phys. Chem. Chem. Phys.* **2000**, *2*, 2291−2296.
(111) Ziessel, R. F.; Ulrich, G.; Charbonnière, L.; Imbert, D.; Scopelliti, R.; Bünzli, J. C. G. NIR Lanthanide Luminescence by Energy Transfer from Appended Terpyridine-Boradiazaindacene Dyes. *Chem. - Eur. J.* **2006**, *12*, 5060−5067.
(112) Nonat, A.; Imbert, D.; Pecaut, J.; Giraud, M.; Mazzanti, M. Structural and Photophysical Studies of Highly Stable Lanthanide Complexes of Tripodal 8-Hydroxyquinolinate Ligands Based on 1,4,7-Triazacyclononane. *Inorg. Chem.* **2009**, *48*, 4207−4218.
(113) Ilmi, R.; Hasan, N.; Liu, J.; Mara, D.; van Deun, R.; Iftikhar, K. Effect of 2,4,6-Tri(2-Pyridyl)-1,3,5-Triazine on Visible and NIR Luminescence of Lanthanide Tris(Trifluoroacetylacetonates). *J. Photochem. Photobiol., A* **2017**, *347*, 116−129.
(114) Nonat, A. M.; Allain, C.; Faulkner, S.; Gunnlaugsson, T. Mixed d-f_3 Coordination Complexes Possessing Improved near-Infrared (NIR) Lanthanide Luminescent Properties in Aqueous Solution. *Inorg. Chem.* **2010**, *49*, 8449−8456.
(115) Hebbink, G. A.; Grave, L.; Woldering, L. A.; Reinhoudt, D. N.; Van Veggel, F. C. J. M. Unexpected Sensitization Efficiency of the Near-Infrared Nd^{3+}, Er^{3+}, and Yb^{3+} Emission by Fluorescein Compared to Eosin and Erythrosin. *J. Phys. Chem. A* **2003**, *107*, 2483−2491.

https://doi.org/10.1021/acs.jpca.2c01052
J. Phys. Chem. A 2022, 126, 2498−2510

(116) Yang, L.; Gong, Z.; Nie, D.; Lou, B.; Bian, Z.; Guan, M.; Huang, C.; Lee, H. J.; Baik, W. P. Promoting Near-Infrared Emission of Neodymium Complexes by Tuning the Singlet and Triplet Energy Levels of β-Diketonates. *New J. Chem.* **2006**, *30*, 791−796.
(117) Cross, J. P.; Lauz, M.; Badger, P. D.; Petoud, S. Polymetallic Lanthanide Complexes with PAMAM-Naphthalimide Dendritic Ligands: Luminescent Lanthanide Complexes Formed in Solution. *J. Am. Chem. Soc.* **2004**, *126*, 16278−16279.
(118) Charbonnière, L. J.; Ziessel, R.; Montalti, M.; Prodi, L.; Zaccheroni, N.; Boehme, C.; Wipff, G. Luminescent Lanthanide Complexes of a Bis-Bipyridine-Phosphine-Oxide Ligand as Tools for Anion Detection. *J. Am. Chem. Soc.* **2002**, *124*, 7779−7788.
(119) Chow, C. Y.; Eliseeva, S.; Trivedi, E. R.; Nguyen, T. N.; Kampf, J. W.; Petoud, S.; Pecoraro, V. L. Ga^{3+}/Ln^{3+} Metallacrowns: A Promising Family of Highly Luminescent Lanthanide Complexes That Covers Visible and Near-Infrared Domains. *J. Am. Chem. Soc.* **2016**, *138*, 5100−5109.
(120) Caillé, F.; Bonnet, C. S.; Buron, F.; Villette, S.; Helm, L.; Petoud, S.; Suzenet, F.; Tóth, É. Isoquinoline-Based Lanthanide Complexes: Bright NIR Optical Probes and Efficient MRI Agents. *Inorg. Chem.* **2012**, *51*, 2522−2532.
(121) Isaac, M.; Raibaut, L.; Cepeda, C.; Roux, A.; Boturyn, D.; Eliseeva, S. V.; Petoud, S.; Sénèque, O. Luminescent Zinc Fingers: Zn-Responsive Neodymium Near-Infrared Emission in Water. *Chem. - Eur. J.* **2017**, *23*, 10992−10996.
(122) Lo, W. S.; Li, H.; Law, G. L.; Wong, W. T.; Wong, K. L. Efficient and Selective Singlet Oxygen Sensitized NIR Luminescence of a Neodymium(III) Complex and Its Application in Biological Imaging. *J. Lumin.* **2016**, *169*, 549−552.

Recommended by ACS

Impact of 1,10-Phenanthroline-Induced Intermediate Valence on the Luminesence of Divalent Europium Halides
Laura C. Straub, Bertold Rasche, *et al.*
DECEMBER 23, 2022
INORGANIC CHEMISTRY
READ

Binuclear Lanthanide Complexes Based on 4-Picoline-*N*-oxide: From Sensitized Luminescence to Single-Molecule Magnet Characteristics
Senthil Kumar Kuppusamy, Mario Ruben, *et al.*
JANUARY 16, 2023
CRYSTAL GROWTH & DESIGN
READ

Properties of Amine-Containing Ligands That Are Necessary for Visible-Light-Promoted Catalysis with Divalent Europium
Ramiro Barraza Jr., Matthew J. Allen, *et al.*
NOVEMBER 23, 2022
INORGANIC CHEMISTRY
READ

Emission Properties of Eu(III) Complexes Containing Arsine and Phosphine Ligands with Annulated Structures
Toshiki Fujii, Kensuke Naka, *et al.*
OCTOBER 27, 2022
INORGANIC CHEMISTRY
READ

Get More Suggestions >

https://doi.org/10.1021/acs.jpca.2c01052
J. Phys. Chem. A 2022, 126, 2498−2510